HHS Public Access

Author manuscript

Eur J Plast Surg. Author manuscript; available in PMC 2018 November 01.

Published in final edited form as:

Eur J Plast Surg. 2017 November ; 40(5): 383–392. doi:10.1007/s00238-017-1308-9.

Characterization of the Foreign Body Response to Common Surgical Biomaterials in a Murine Model

Mohamed Ibrahim, MD[1], **Jennifer Bond, PhD**[1], **Manuel A. Medina, MD**[1], **Lei Chen, MD**[3], **Carlos Quiles, MD**[1], **George Kokosis, MD**[1], **Latif Bashirov, MD**[1], **Bruce Klitzman, PhD**[1,2], and **Howard Levinson, MD**[1,2]

[1]Division of Plastic and Reconstructive Surgery, Department of Surgery, Duke University School of Medicine, Durham NC

[2]Department of Biomedical Engineering, Duke University, Durham NC

[3]Department of Burn Surgery, the First Affiliated Hospital of Sun Yat-sen University, Guangzhou, Guangdong, China

Abstract

Background—Implanted biomaterials are subject to a significant reaction from the host, known as the foreign body response (FBR). We quantified the FBR to five materials following subcutaneous implantation in mice.

Materials and methods—Polyvinyl alcohol (PVA) and silicone sheets are considered highly biocompatible biomaterials and were cut into 8mm-diameter disks. Expanded PTFE (ePTFE)and polypropylene are also widely used biocompatible biomaterials and were cut into 2cm-long cylinders. Cotton was selected as a negative control material that would invoke an intense FBR, was cut into disks and implanted. The implants were inserted subcutaneously into female C57BL/6 mice. On post-implantation days 14, 30, 60, 90 and 180, implants were retrieved. Cellularity was assessed with DAPI stain, collagen with Masson's trichrome stain. mast cells with toluidine-blue, macrophages with F4/80 immunohistochemical-stain, and capsular thickness and foreign body giant cells with hematoxylin & eosin.

Results—DAPI revealed a significantly increased cellularity in both PVA andsilicone, and ePTFE had the lowest cell density. Silicone showed the lowest cellularity at d14 and d90 whereas ePTFE showed the lowest cellularity at days 30, 60, and 180. Masson's trichrome staining demonstrated no apparent difference in collagen. Toluidine blue showed no differences in mast cells. There were, however, fewer macrophages associated with ePTFE. On d14, PVA had highest

Corresponding author: Howard Levinson, MD, Division of Plastic and Reconstructive Surgery, Department of Surgery, Duke University School of Medicine, Durham, North Carolina, USA, howard.levinson@duke.edu.

Ethical Statement:

All animal procedures were performed in accordance with an Institutional Animal Care and Use Committee (IACUC) protocol approved by the Duke University.

The authors report no proprietary or commercial interest in any product mentioned or concept discussed in this article.
This work was supported by a grant from the National Institutes of Health, K08 GM 085562-05.

Disclosure

The authors report no proprietary or commercial interest in any product mentioned or concept discussed in this article.
This work was supported by a grant from the National Institutes of Health, K08 GM 085562-05.

number of macrophages, whereas polypropylene had the highest number at all time points after d14. Giant cells increased earlier and gradually decreased later. On d90, PVA exhibited a significantly increased number of giant cells compared to polypropylene and silicone. Silicone consistently formed the thinnest capsule throughout all time points. On d14, cotton had formed the thickest capsule. On d30 polypropylenehas formed thickest capsule and on days 60, 90 and 180, PVA had formed thickest capsule.

Conclusion—These data reveal differences in capsule thickness and cellular response in an implant-related manor, indicating that fibrotic reactions to biomaterials are implant specific and should be carefully considered when performing studies on fibrosis when biomaterials are being used.

Keywords

implants; biocompatibility; fibrosis; PVA; ePTFE; Prolene; polypropylene

Introduction

Implanted biomaterials elicit a significant reaction from the host, known as the foreign body response (FBR). The FBR is initiated by the innate immune response prompted by adhesion of proteins and other biomolecules to the surface of the implant[1] followed by macrophage recruitment and tissue inflammation. Dissolution, degradation, or even complete phagocytosis of foreign objects resolves the FBR and normal wound healing is restored.[2] Implants with prolonged tissue residence develop a relatively avascular collagen-rich capsule around the implant, which sequesters it from the surrounding tissue.[3] The intensity and impact of the FBR depends upon recruitment and reactivity of several cell mediators. This intensity of the inflammatory response is mainly determined by the characteristics and composition of the implanted material.

The cells involved in the FBR have a specific role in modulating the local tissue response, thus affecting subsequent healing, including chronic inflammation and the FBR.[2] Early in the inflammatory process, mast cells (MC) are recruited through chemotactic inflammatory signaling to wound sites where they mature and activate. Activated MC secrete mediators such as IL-4 and IL-13, which provide chemotactic signals that recruit macrophages. MC also secrete histamine and serotonin causing vasodilation which facilitates greater access to the inflammatory cells arriving at the wound site.[1]

Macrophages ef ciently clean the wound site of microscopic particles, bacteria and dead cells through phagocytosis, however; they are unable to digest macroscopic implants, leading to chronic in ammation. To increase their effectiveness, macrophages undergo fusion to form foreign body giant cells (FBGC) that can perpetually remain at the tissue/implant interface.[4] Still unsuccessful in their attempt to digest the implant, FBGCs secrete cytokines that trigger broblasts to deposit a collagen capsule around the implant to permanently sequester it from the surrounding tissue.[2]

Biomaterials have been created for varying medical applications. Whether biologic or synthetic, the material’s physical and chemical properties govern its use and application.

PVA sponges have several applications, one of which is in wound healing. Due to its topography and porous composition it can be used in chronic wound care. Serving as a bacteriostatic dressing it functions as a drug delivery vehicle, tool for debridement and a sponge for excess fluid in the wound bed.[5] As a research tool, the polyvinyl alcohol sponge (PVA) is useful for analyzing granulation tissue formation, collagen deposition, wound fluid composition, and the effects of substances on the healing process.[6] In addition to its use in studying a wide array of attributes of wound healing, it has also been utilized to investigate tumor angiogenesis, drug delivery and stem cell survival. [1,7,8]

Expanded polytetrafluoroethylene (ePTFE), is particularly attractive for human use and has become one of the most frequently used because it is safe. Clinically, ePTFE is being used in vascular grafts.[9] Capable in aiding measurement of inflammation, fibroplasia, and matrix deposition, it is employed as a research tool. Because small vessels also penetrate its interstices, it is potentially capable of measuring angiogenesis. It can also be used to sample live tissue for measurement under culture conditions.[10,11] This model has been extensively and successfully used by us and others in human and animal studies.[12]

Polypropylene (Prolene) mesh is routinely used for hernia repair, resistant to mechanical stress, relatively inert, and well-tolerated by patients.[13] It induces chronic inflammation and fibrosis which are the therapeutic strategy of this material.[14] Subcutaneous cotton has been used as an irritant to induce granulomas and chronic inflammation in several animal models.[15] Polydimethylsiloxane (silicone) has been considered to be an immunologically inert material,[16] it is widely used for many surgical interventions e.g. breast implants and maxillofacial prosthetic materials.[17,18] Here, we evaluate the FBR to different biomedical implants and the possible utilization of these materials to be used as fibrosis models to further study diagnostic and therapeutic applications.

Materials and Methods

All animal procedures were performed in accordance with an Institutional Animal Care and Use Committee (IACUC) protocol approved by the Duke University.

Mice

Female C57BL/6 mice, 10–12 weeks-old, weighing 18 to 23 g (Jackson Laboratories, Bar Harbor, ME), were used throughout the study. Three mice were used for each type of implant evaluated, for each time point. All mice were monitored for signs of toxicity including significant weight change, grooming, irritability and respiratory rate. The mice were housed under protocols approved by the Institutional Animal Care and Use Committee (IACUC) of Duke University.

Implanted materials

Five materials of subcutaneous implants were used: 1) PVA sponge (PVA Unlimited, Warsaw, IN), 2) polypropylene nonabsorbable synthetic surgical mesh (Ethicon, Cornelia, GA), 3) expanded polytetrafluoroethylene (ePTFE) tubes (International Polymer Engineering, Tempe, AZ), 4) cotton sheets (Target, Minneapolis, MN), and 5) silicone sheets (Invotec International, Jacksonville, FL). The synthetic PVA, cotton and silicone sheets were

cut into 8mm diameter disks. ePTFE and polypropylene were cut into 2cm-long tubes. All materials were sterilized by autoclaving. (Figure 1)

Surgical procedures

All procedures were performed in accordance with a protocol approved by the Duke University IACUC. Mice were anesthetized using gas anesthesia (O_2, 2L/min, isoflurane, 2%). After induction of anesthesia, the surgical site was shaved and sterilized. An incision was created in the skin described: PVA, cotton and silicone implants: an 8mm incision was made and a subcutaneous pocket was created at incision by blunt dissection. For Prolene, and ePTFE, a 3mm long incision was made and a subcutaneous pocket was created at incision by blunt dissection. Each implant was inserted into each pocket. The incision was closed with 5-0 silk sutures. The mice were monitored until fully recovered from anesthesia. (Figure 1)

Tissue collection

On days 14, 30, 60, 90 and 180 the implants were retrieved with the surrounding capsule and tissue. The retrieved tissue samples were fixed in 10% buffered formalin, embedded in paraffin, and sectioned for histology (5μm thick). After implants retrieval, the mice were euthanized by intraperitoneal injection of EUTHASOL® (Virbac, Fort Worth, TX) solution.

Hematoxylin and eosin staining

Tissue sections were deparaf nized in the oven at 65°C overnight, immersed in xylene for 15-min, dehydrated with decreasing concentrations of absolute alcohol, and then hydrated with distilled water. They were then immersed in Mayer's hematoxylin solution for 5min and then washed with tap water for 20min; the sections were then counterstained with eosin for 35s. Finally, sections were dehydrated with increasing concentrations of absolute alcohol, cleared in xylene, and mounted in Richard-Allan Scientific Cytoseal™ 60 mounting medium. Images were captured using a Nikon eclipse E600 microscope.

Masson's trichrome staining

The sections were placed in Biebrich scarlet-acid Fuchsin solution for 5min, washed with distilled water, and placed in Phosphomolybdic-Phosphotungstic acid solution for 5min. The sections were placed in Aniline Blue solution for 5min after which they were placed in 1% acetic acid solution for 2min before they were washed with distilled water. Finally, sections were dehydrated with increasing concentrations of absolute alcohol, cleared in xylene, and mounted in Richard-Allan Scientific Cytoseal™ 60 mounting medium. Images were captured using a Nikon eclipse E600 microscope. The color information from each HPF image was quantified using colorimetric analysis. The collagen index value was calculated as collagen index = (B + G)/(2R + B + G) for each pixel within the image (where R, G, and B represent the red, blue, and green pixel values, respectively).[19] The value of the collagen index ranged from 0 for extremely red objects to 1 for completely blue-green objects. The average collagen index of 3 high power field (HPF) images for each time point was graphed.

DAPI staining

DAPI (4′, 6-diamidino-2-phenylindole) is a fluorescent nuclear counterstain. The sections were mounted in Vectashield ® mounting medium with DAPI. Stained nuclei were visualized by use of a Nikon eclipse E600 microscope and images were captured with a Nikon DXM 1200 digital camera under the same settings. Five HPF images were analyzed from each tissue section and the average number of cells was assayed.

Toluidine blue staining

Toluidine blue stock solution composed of 1g of Toluidine blue O (Sigma-Aldrich) mixed in 100 ml of 70% alcohol. Finally, sections were dehydrated with increasing concentrations of absolute alcohol, cleared in xylene, and mounted in Richard-Allan Scientific Cytoseal™ 60 mounting medium. Labeled mast cells were visualized by use of a Nikon eclipse E600 microscope and images were captured with a Nikon DXM 1200 digital camera under the same settings. Five HPF images were analyzed from each tissue section and the average number of mast cells was assayed.

Macrophage F4/80 staining

Sections immersed in 3% hydrogen peroxide (H_2O_2) for 10min to inhibit endogenous peroxidase. Slides were placed into citrate pH 6 antigen retrieval solution (Target Retrieval Solution, Dako North America Inc. Carpinteria, CA, USA) and brought to >85°C in a water bath for 20min, followed by 30min cool down. After rinsing sections with deionized water and 1X Tris-buffered saline (TBS, TBS Automation Washing Buffer, Biocare Medical, Concord, CA, USA), sections were treated with 10% goat serum (Normal Goat Serum, Vector Laboratories, Burlingame, CA, USA) for 1h at room temperature to block non-specific antibody binding. F4/80 (at a 1:1500 dilution, eBioscience, San Diego, CA, USA) was incubated for 1h at room temperature. After washing with TBS, the slides were incubated with biotinylated rabbit anti rat (1:200 dilution, Vector Laboratories, Burlingame, CA, USA) for 30min at room temperature. The sections were then incubated with avidin-biotin complex reaction (Vector Laboratories, Burlingame, CA, USA) for 30min. The slides were incubated with DAB substrate solution for 3min after rinsing with 1X TBS. The slides were quickly dipped in hematoxylin solution for counter stain solution, and then were rinsed in running tap water for 20min. After dehydration, labeled cells were visualized by use of a Nikon eclipse E600 microscope and images were captured with a Nikon DXM 1200 digital camera under the same settings. Five HPF images were analyzed from each tissue section and the average number of cells was assayed.

Capsular thickness and FBGC

Quantitative measurements were provided examining the width of each capsule on the superficial and deep sides of the graft. Three to 4 measurements were taken from each side of the implant per slide. These measurements were averaged to create a mean thickness of each implant from 8 to 12 measurements. The thickness of the fibrous capsule was measured in mm using ImageJ software (National Institutes of Health, Bethesda, MD, USA). FBGCs were quantified by examining five HPF images from each tissue section and the average number of cells was assayed.

Statistical analysis

Data were analyzed using Microsoft® Excel software. The statistical signi cance of values among groups was evaluated by the analysis of variance (ANOVA), followed by least signi cant difference *t*-test. All values used in figures and text are expressed as mean +/− standard error of the mean (SEM). The difference was considered signi cant when the p-value was 0.05 or less.

Results

Gross Analysis

Neither tissue necrosis nor abscess formation was observed around the implanted materials on gross examination. All implanted materials remained in the original implantation site without signs of infection or rejection. All materials were grossly intact and the surrounding connective tissue showed no calcifications. Table 1 summarizes the histological findings.

Cellularity

DAPI-stained sections of implants and surrounding tissue revealed significant increases in cellular infiltration in PVA at all time points compared to other implanted materials ($p<0.05$). Silicone showed the least cellularity at days 14 and 90 whereas ePTFE showed the least cellularity in days 30, 60, and 180. Other implanted materials showed varying degrees of cellularity at different time points (Figure 2).

Collagen Index

Histological analysis of Masson's trichrome-stained sections demonstrated no statistically significant change between the implants in different time points, however; PVA and cotton have demonstrated a relative increase in collagen index compared to other implants. ePTFE and silicone had relatively lower collagen index. (Figure 3)

Mast Cells

Histological analysis of Toluidine blue-stained sections showed varying increases in mast cell numbers between different implants at different time points, however; none of these increases were statistically significant. On day 14, ePTFE showed the highest number of mast cells whereas cotton showed the least. On day 30, ePTFE also showed the highest number of mast cells whereas PVA showed the least. On day 60, cotton showed the highest number of mast cells whereas silicone showed the least. On day 90, ePTFE demonstrated the highest number of mast cells whereas silicone was still the least. On day 180, PVA showed the highest number of mast cells whereas cotton showed the least (Figure 4).

Macrophages

Immunohistochemistry using F4/80 as a marker, demonstrated cells of positive macrophage staining in the implants and the surrounding capsules. ePTFE has demonstrated significantly decreased number of macrophages in all time points compared to the other implanted materials. In day 14, PVA has demonstrated the highest number of macrophages compared

to other implants, whereas Prolene demonstrated the highest number of macrophages at all time points after day 14. (Figure 5)

Giant cells

Giant cells increased at earlier time points and gradually decreased at later time points in all groups. There was no statistically significant difference in the numbers of giant cells between different implants at all time points except in day 90, where PVA has shown significantly increased number of giant cells compared to Prolene and silicone. (Figure 6)

Capsular thickness

All materials were surrounded by capsules, which were measured as previously described. Silicone consistently formed the thinnest capsule throughout all the time points. On day 14, cotton formed the thickest capsule, on day 30 Prolene formed the thickest capsule, whereas on days 60, 90 and 180, PVA formed the thickest capsule (Figure 7).

Discussion

Surgical implantation of biomaterials triggers a series of host reactions at the implantation site that include interactions material/tissue, inflammation, granulation tissue development, foreign body reaction, and fibrosis and fibrous capsule formation.[20] The normal physiological response to implanted biomaterials is the FBR.[21] Implanted materials produce an initial acute inflammatory response followed by a chronic fibro-proliferative response.[22] Biocompatibility of implanted materials is determined by the intensity of these responses and the ability to resolve injury to the tissues during implantation. Overall, this study demonstrated that PVA and Prolene elicited a more robust inflammatory response and FBR, than cotton, silicone and ePTFE.

In the present study, all implanted biomaterials elicited an inflammatory response and FBR with varying degrees of severity. DAPI is a non-specific global marker that stains all nuclei, although it cannot differentiate types of cells, it is still helpful in providing an overall indicator of the cellular infiltration to the implants, thus, we have further supported the analysis through using specific inflammatory cells markers. Our DAPI analysis demonstrated that all biomaterials have promoted cellular infiltration with PVA demonstrating the most cellular infiltration at all time points (Figure 2), indicating an overall increased FBR to PVA compared to other implanted biomaterials. The increased cellular infiltration could be explained by the histaminic responses elicited through the biomaterials in the surrounding tissue, and histamine is known to increase capillary permeability and promote rapid diapedesis of inflammatory cells into target tissue.[23] Our evaluation of the presence of mast cells in the biomaterial implants revealed that all biomaterials exhibit persistently elevated numbers of mast cells at all time points. However, none of the implants showed significant differences when compared to each other (Figure 4). Mast cell degranulation mediates acute inflammatory responses to implanted biomaterials and plays a significant role in macrophage recruitment and degree of subsequent FBR.[24]

The FBR impacts biomaterials by altering their biocompatibility.[1] The FBR is composed of many other inflammatory cells, including macrophages and is the end-stage response of

inflammatory and wound healing responses.[1] Our study has demonstrated the presence of macrophages in all biomaterial implants at all time points. PVA and prolene demonstrated a significantly increased number of macrophages compared to other implanted biomaterials reflecting a more robust FBR (Figure 5). Failure of the macrophages to engulf the implanted biomaterials resulted in the formation of multinucleated giant cells that surround the material.[25] In indigestible materials, multinucleated giant cells promote the formation of a thick fibrous capsule which minimizes further reactivity. The extent of capsule formation is related to implant surface chemistry and surface area.[26] Not surprisingly, in this study, silicone consistently formed the thinnest capsule throughout all the time points, whereas PVA and Prolene formed the thickest capsule, as described in the results. This study has also demonstrated the presence of multinucleated giant cells in all implanted materials at all time points. Multinucleated giant cells numbers progressively decrease over time so that day 180 showed the least number of multinucleated giant cells in all implanted materials (Figure 6).

To understand the difference in the FBR between different implants, it is important to realize that the reaction of cells and tissues to implanted foreign bodies depends on the material's properties and its behavior upon contact with the host tissue.[27] Surface topography and texture of the implanted material, also contributes to the intensity of the FBR.[27] Previous reports indicated that encapsulation is influenced by many factors, including properties of the biomaterial, biomaterial porosity, surface texture, and implantation site.[28] We have not objectively assessed or quantified the properties of the materials we have used in this study, however the subjective gross assessment of these materials and our results are consistent with previous reports that the intensity of the FBR correlates with the properties of each biomaterial. The shape and the design of the biomaterial can influence the FBR, through stretching of the surrounding tissue, in this study we could not use the same shape for all the biomaterials due to the difference in the properties of each material, however, we do not think that this was a true limitation of the study because even though ePTFE and Prolene were both implanted as tubes, they elicited very different FBR that is more consistent with the properties of their materials, the same could also be said about disk-shaped materials; PVA, cotton and silicone. Overall, PVA, cotton and Prolene had shown a robust FBR whereas silicone and ePTFE had shown the least FBR at most time points (Table 1).

Conclusions

In the present study, we compared the FBR of five different commonly used biomedical implants. Overall, PVA demonstrated the highest cellularity whereas ePTFE and silicone were the least cellular. No statistically significant differences in collagen index and mast cell infiltration were observed between implants. Prolene and PVA demonstrated the highest degree of macrophage infiltration, whereas ePTFE had the least. Giant cells were present in all implants and were not statistically significant different between implants. Silicone has consistently formed the thinnest capsule. On day 14, cotton formed the thickest capsule, on day 30 prolene formed the thickest capsule whereas on days 60, 90 and 180, PVA formed the thickest capsule. These findings help to understand the foreign body response of the compared materials.

Acknowledgments

The authors would like to thank Gloria Adcock for her assistance with tissue processing.

References

1. Sprugel KH, McPherson JM, Clowes AW, Ross R. Effects of growth factors in vivo. I. Cell ingrowth into porous subcutaneous chambers. The American journal of pathology. 1987; 129:601–613. [PubMed: 3501246]
2. Anderson JM, Rodriguez A, Chang DT. Foreign body reaction to biomaterials. Seminars in immunology. 2008; 20:86–100. [PubMed: 18162407]
3. Avula M, Rao AN, McGill LD, Grainger DW, Solzbacher F. Foreign Body Response To Subcutaneous Biomaterial Implants in a Mast Cell-deficient Kit Murine Model. Acta biomaterialia. 2014
4. Nichols SP, et al. The effect of nitric oxide surface flux on the foreign body response to subcutaneous implants. Biomaterials. 2012; 33:6305–6312. [PubMed: 22748919]
5. McNally AK, Jones JA, Macewan SR, Colton E, Anderson JM. Vitronectin is a critical protein adhesion substrate for IL-4-induced foreign body giant cell formation. Journal of biomedical materials research. Part A. 2008; 86:535–543. [PubMed: 17994558]
6. Xie Z, et al. Dual growth factor releasing multi-functional nanofibers for wound healing. Acta biomaterialia. 2013; 9:9351–9359. [PubMed: 23917148]
7. Davidson JM. Animal models for wound repair. Archives of dermatological research. 1998; 290(Suppl):S1–11. [PubMed: 9710378]
8. Alfaro MP, et al. sFRP2 suppression of bone morphogenic protein (BMP) and Wnt signaling mediates mesenchymal stem cell (MSC) self-renewal promoting engraftment and myocardial repair. The Journal of biological chemistry. 2010; 285:35645–35653. [PubMed: 20826809]
9. Andrade SP, Ferreira MA. The sponge implant model of angiogenesis. Methods in molecular biology. 2009; 467:295–304. [PubMed: 19301679]
10. Wallusche ck KP, Bierkandt S, Brandt M, Cremer J. Infrainguinal ePTFE vascular graft with bioactive surface heparin bonding. First clinical results. The Journal of cardiovascular surgery. 2005; 46:425–430. [PubMed: 16160689]
11. Adzick NS, et al. Comparison of fetal, newborn, and adult wound healing by histologic, enzyme-histochemical, and hydroxyproline determinations. Journal of pediatric surgery. 1985; 20:315–319. [PubMed: 4045654]
12. Goodson WH 3rd, Hunt TK. Wound collagen accumulation in obese hyperglycemic mice. Diabetes. 1986; 35:491–495. [PubMed: 3514328]
13. Goodson WH 3rd, et al. The influence of a brief preoperative illness on postoperative healing. Annals of surgery. 1987; 205:250–255. [PubMed: 3827360]
14. Orenstein SB, Saberski ER, Kreutzer DL, Novitsky YW. Comparative analysis of histopathologic effects of synthetic meshes based on material, weight, and pore size in mice. The Journal of surgical research. 2012; 176:423–429. [PubMed: 22099590]
15. Junge K, et al. Mesh biocompatibility: effects of cellular inflammation and tissue remodelling. Langenbeck's archives of surgery/Deutsche Gesellschaft fur Chirurgie. 2012; 397:255–270.
16. Rassaert CL, Dipasquale G, O'Donoghue S. The evaluation of cotton twine as a new anti-inflammatory assay. Agents and actions. 1975; 5:128–132. [PubMed: 1155301]
17. Heggers JP, et al. Biocompatibility of silicone implants. Annals of plastic surgery. 1983; 11:38–45. [PubMed: 6614755]
18. Franca DC, de Castro AL, Soubhia AM, de Aguiar SM, Goiato MC. Evaluation of the biocompatibility of silicone gel implants - histomorphometric study. Acta informatica medica: AIM: journal of the Society for Medical Informatics of Bosnia & Herzegovina: casopis Drustva za medicinsku informatiku BiH. 2013; 21:93–97. [PubMed: 24039333]
19. Franca DC, et al. Biocompatibility evaluation of 3 facial silicone elastomers. The Journal of craniofacial surgery. 2011; 22:837–840. [PubMed: 21558944]

20. Olbrich KC, et al. Halofuginone inhibits collagen deposition in fibrous capsules around implants. Annals of plastic surgery. 2005; 54:293–296. discussion 296. [PubMed: 15725837]
21. Morehead JM, Holt GR. Soft-tissue response to synthetic biomaterials. Otolaryngologic clinics of North America. 1994; 27:195–201. [PubMed: 8159421]
22. Ziats NP, Miller KM, Anderson JM. In vitro and in vivo interactions of cells with biomaterials. Biomaterials. 1988; 9:5–13. [PubMed: 3280039]
23. Tang L, Jennings TA, Eaton JW. Mast cells mediate acute inflammatory responses to implanted biomaterials. Proceedings of the National Academy of Sciences of the United States of America. 1998; 95:8841–8846. [PubMed: 9671766]
24. Zdolsek J, Eaton JW, Tang L. Histamine release and fibrinogen adsorption mediate acute inflammatory responses to biomaterial implants in humans. Journal of translational medicine. 2007; 5:31. [PubMed: 17603911]
25. Carr BJ, Ochoa L, Rankin D, Owens BD. Biologic response to orthopedic sutures: a histologic study in a rabbit model. Orthopedics. 2009; 32:828. [PubMed: 19902886]
26. Anderson JM. Multinucleated giant cells. Current opinion in hematology. 2000; 7:40–47. [PubMed: 10608503]
27. Ratner BD. Reducing capsular thickness and enhancing angiogenesis around implant drug release systems. Journal of controlled release: official journal of the Controlled Release Society. 2002; 78:211–218. [PubMed: 11772462]
28. Rompen E, Domken O, Degidi M, Pontes AE, Piattelli A. The effect of material characteristics, of surface topography and of implant components and connections on soft tissue integration: a literature review. Clinical oral implants research. 2006; 17(Suppl 2):55–67. [PubMed: 16968382]

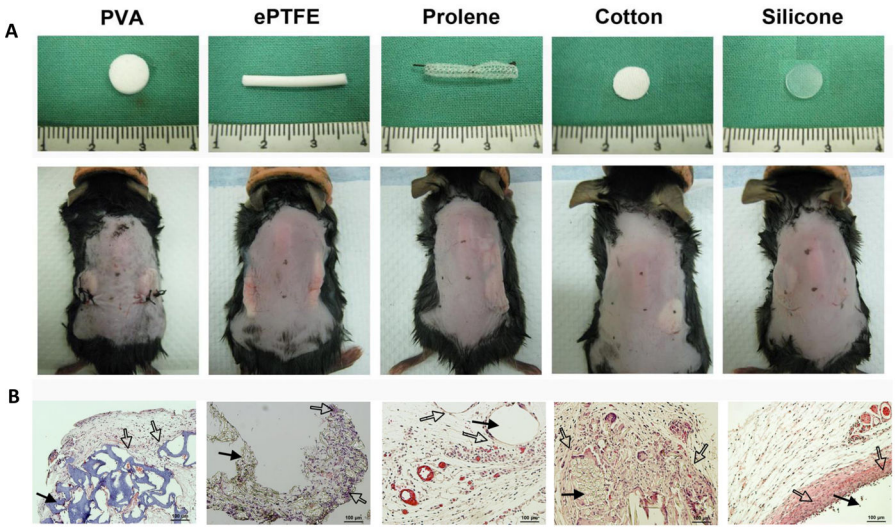

Figure 1.

(A) Gross view of the implanted material before and after implantation. *(B)* H&E-stained section of the implant material (**solid arrow**) and the surrounding capsule (**hollow arrows).**

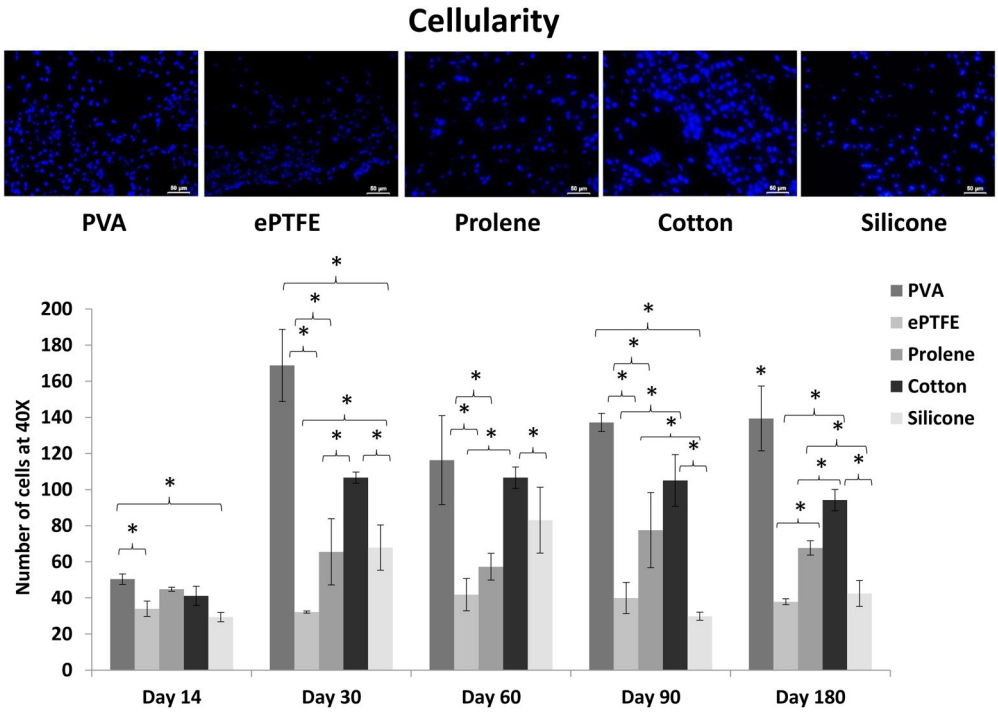

Figure 2.

Representative DAPI-stained section of the implants demonstrating cellularity. Quantitative analysis of DAPI stained-sections is graphically represented. The average number of cells in 5 HPFs of 3 samples for each time point was graphed. Values are represented as mean±SEM. $^{*}P<0.05$

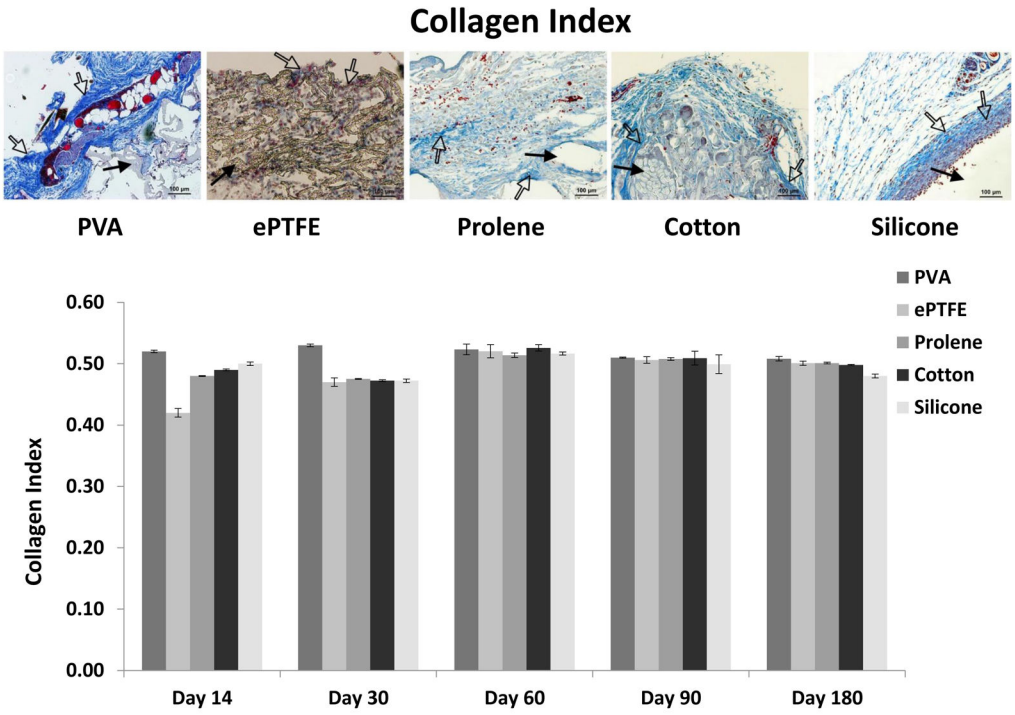

Figure 3.

Masson-stained sections show the material of the implant (**Solid arrow**) and the collagen distribution (**Hollow arrows**). Scale bar = 100 μm.

Quantitative analysis of collagen index is graphically represented. No statistically significant difference between implants.

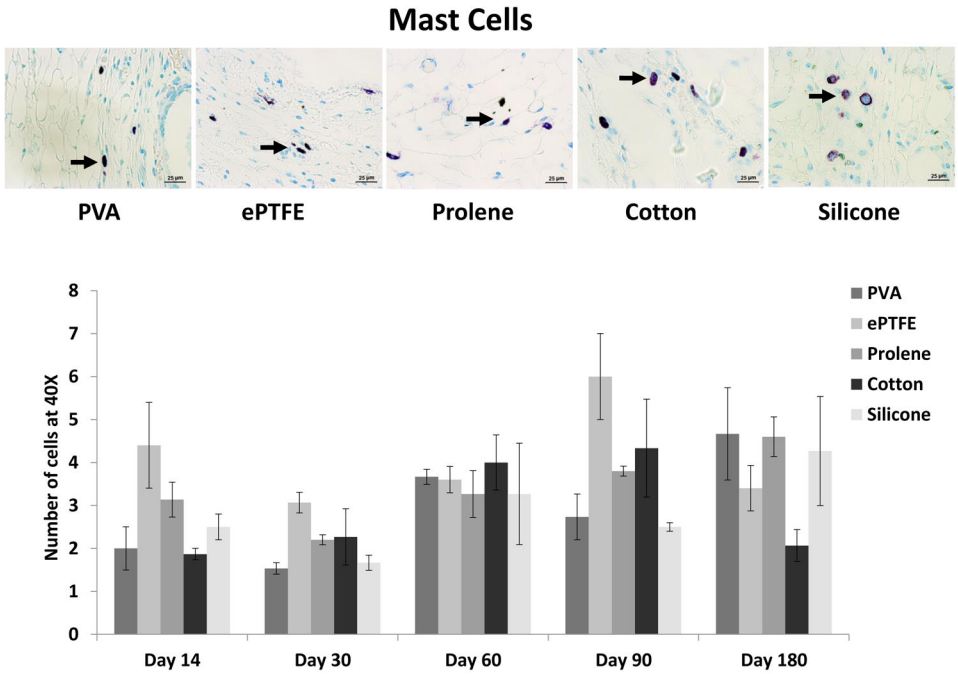

Figure 4.

Toluidine-blue sections show the mast cells (**arrow**). Scale bar = 25 μm. Quantitative analysis of mast cell density index is graphically represented. The average number of cells in 5 HPFs of 3 samples for each time point was graphed. Values are represented as mean±SEM. No statistically significant difference between implants.

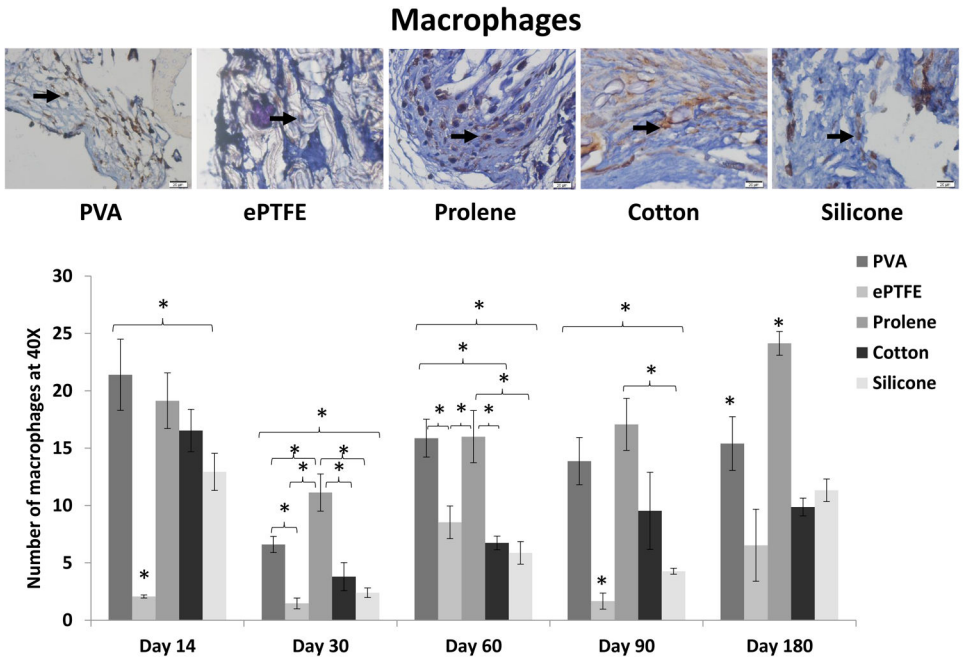

Figure 5.

F4/80 immune-stained sections show the macrophages (**arrow**). Scale bar = 25 μm. Quantitative analysis of macrophage density is graphically represented. The average number of cells in 5 HPFs of 3 samples for each time point was graphed. Values are represented as mean±SEM. $^{*}P<0.05$

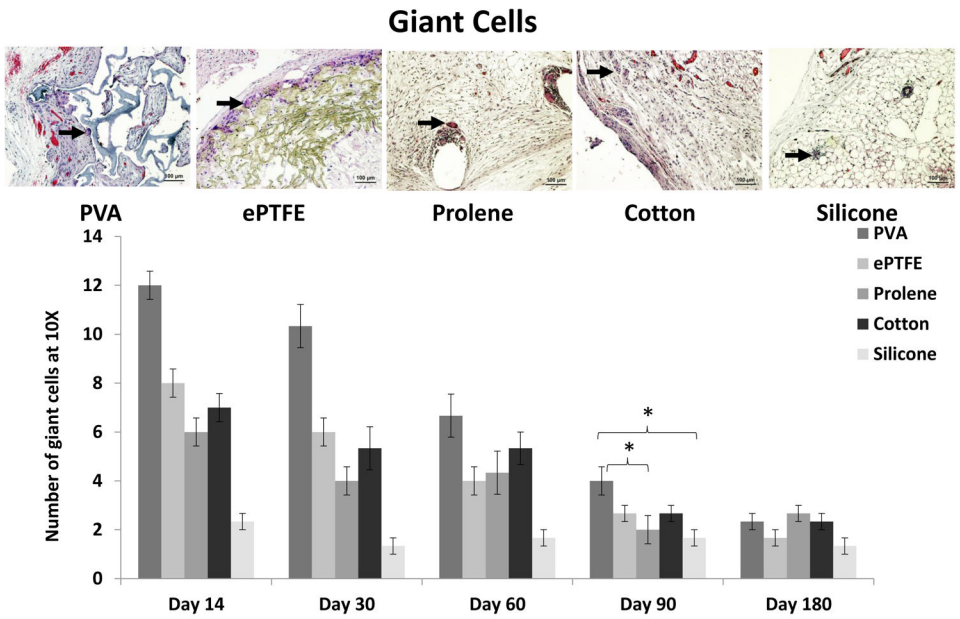

Figure 6.

H&E-stained sections show the giant cells (**arrow**). Scale bar = 100 μm.

Quantitative analysis giant cells is graphically represented. The average number of cells in 5 fields of 3 samples for each time point was graphed. Values are represented as mean ±SEM. $^{*}P<0.05$

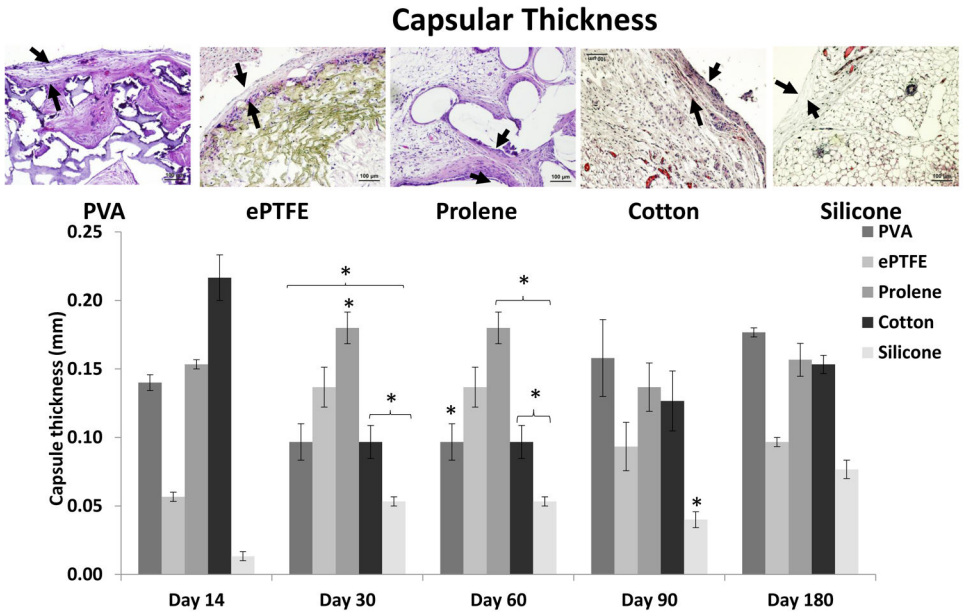

Figure 7.

H&E-stained sections show capsules (**between arrows**). Scale bar = 100 μm. Quantitative measurements were provided examining the width of each capsule on the superficial and deep sides of the implant. Three to 4 measurements were taken from each side of the implant per slide. These measurements were averaged to create a mean thickness of each implant from 8 to 12 measurements. Values are represented as mean±SEM. $^{*}P<0.05$

Table 1

Parameter		Day 14	Day 30	Day 60	Day 90	Day 180
Cellularity/HPF	**Highest**	PVA 50±3	PVA 169±32	PVA 116±25	PVA 137±5	PVA 139±18
	Lowest	Silicone 29±3	ePTFE 32±1	ePTFE 42±9	Silicone 30±2	ePTFE 38±2
Collagen Index	**Highest**	PVA 0.52±0.002	PVA 0.53±0.002	Cotton 0.52±0.005	PVA 0.51±0.001	PVA 0.5±0.003
	Lowest	ePTFE 0.42±0.006	ePTFE 0.47±0.006	Prolene 0.51±0.003	Silicone 0.49±0.01	Silicone 0.48±0.003
Mast cells/HPF	**Highest**	ePTFE 4±2	ePTFE 3±0	Cotton 4±1	ePTFE 6±1	PVA 5±1
	Lowest	Cotton 2±0	PVA 2±0	Silicone 3±1	Silicone 3±0	Cotton 2±0
Macrophages/HPF	**Highest**	PVA 21±3	Prolene 11±2	Prolene 16±2	Prolene 17±2	Prolene 24±1
	Lowest	ePTFE 2±0	ePTFE 1±0	ePTFE 9±1	ePTFE 2±1	ePTFE 7±3
Giant cells/HPF	**Highest**	PVA 12±1	PVA 10±1	PVA 7±1	PVA 4±1	Prolene 3±0
	Lowest	Silicone 2±0	Silicone 1±0	Silicone 2±0	Silicone 2±0	Silicone 1±0
Capsular thickness(mm)	**Highest**	Cotton 0.22±0.02	Prolene 0.18±0.01	PVA 0.19±0.02	PVA 0.16±0.03	PVA 0.18±0
	Lowest	Silicone 0.01±0	Silicone 0.05±0	Silicone 0.07±0.01	Silicone 0.04±0.01	Silicone 0.08±0.01